Fundamental relationship of excitonic photoluminescence intensity with excitation density in semiconductor quantum well structures

S. R. Jin[a] M. Ramsteiner, H. T. Grahn, and K. H. Ploog
Paul-Drude-Institut für Festkörperelektronik, Hausvogteiplatz 5-7, D-10117 Berlin, Germany

Z. H. Li, D. X. Shen, and Z. Q. Zhu
Shanghai Institute of Metallurgy, Chinese Academy of Sciences, Shanghai 200050, People's Republic of China

(Received 20 January 2000; accepted for publication 13 July 2000)

The fundamental relationship between excitonic photoluminescence (PL) intensity and excitation intensity in semiconductor quantum well structures is developed. This relationship is further simplified in the regime of low excitation, and used for a fit function of the Arrhenius plot of time-integrated PL intensity. The proposed four fit parameters are definitely correlated to the distinct characteristic quantities of the sample material, which are the binding energy of excitons, the activation energy, the scattering time, and the background concentration in the well. The validity of the model has been confirmed using our experiments. © *2000 American Institute of Physics.* [S0021-8979(00)02220-9]

I. INTRODUCTION

Recombination dynamics in semiconductor quantum well structures has been considerably studied in recent years both theoretically and experimentally.[1–7] It is well known that free excitons and free holes coexist at a certain temperature in the quantum well materials. The photoemission of free excitons plays a dominant role in the low temperature range and can be observed even at room temperature due to the enhanced exciton effect in the wells.

Theoretical study shows that the relative populations of free excitons and free carriers follow well the two-dimensional (2D) law of mass action (i.e., Saha equation).[8,9] It is trivial but possible to distinguish the relative population of free excitons and free carriers using a line-shape analysis, as several authors reported.[10,11] It has also demonstrated the strong dependence of the relative population and consequently the decay time constant of PL intensity on the background concentration of the quantum well materials.[12] Even the intersubband scattering rate can be influenced by excitation density resulting from carrier–carrier interaction. This explains why most of the results of either lifetime or scattering time obtained up to date by different groups sometimes are rather conflicting.

On the other hand, in recombination dynamics of free excitons and free carriers, nonradiative recombination plays a significant role, especially at higher temperatures. Several simplified nonradiative channels have been identified in quantum well structures, such as the either unipolar[13] or bipolar[7,14] thermal escape of hot carriers out from the well into the barriers and then recombination near the interfaces outside the active layer where larger misfit dislocations as well as impurities and defects are expected, or the relaxation by emission of multi-phonons through deep-level centers.[15] For most of the material systems, it is still difficult to reveal the detailed mechanism that actually occurred inside the materials. However, since the experimentally observed temperature behavior related to the nonradiative channels at higher temperatures is usually mono-exponential, it is then possible to extract the activation energy from the Arrhenius plot of time-integrated PL intensity and use it to characterize the predominant nonradiative channel.[15]

In fact, the two thermal processes, i.e., the thermal ionization of free excitons in the low temperature regime and the activation of the nonradiative channels at higher temperature, have significant influence on the optical properties of semiconductor quantum well structures. They result in the reduction and the quenching of excitonic PL emissions. In this article, we present a systematic investigation of temperature dependence of excitonic PL intensity in semiconductor quantum well structures. Both radiative and nonradiative recombinations have been taken into account. Under steady-state condition, the fundamental relationship between excitonic PL intensity and excitation intensity is developed. In the regime of low excitation, the relationship is further simplified and a new fit function is then proposed based on it.

II. THEORETICAL MODEL

Since the thermal processes are much faster than both radiative and nonradiative recombination processes in the temperature range we consider, the dynamic thermal equilibrium is always set up between free excitons and free carriers even under photoexcitation or carrier injection. According to the law of mass action,[8,9] we have the relationship between the populations of free excitons and free electron-hole pairs in the nondegeneate materials

$$\frac{np}{n_x} = n_c, \tag{1}$$

[a]Present address: Physics Department, University of Surrey, Guildford, GU2 5XH, UK; electronic mail: s.jin@surrey.ac.uk

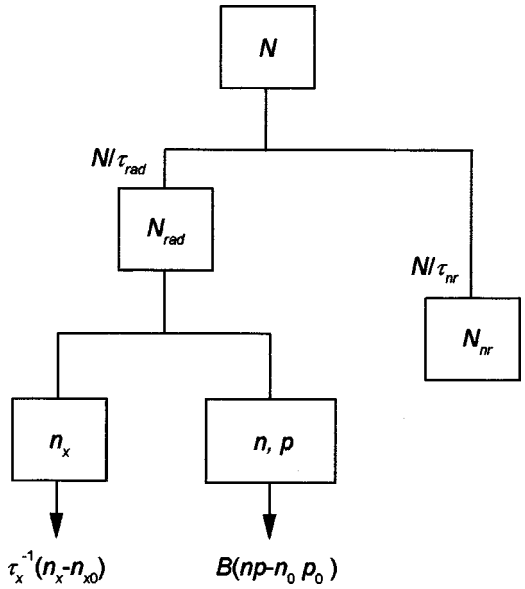

FIG. 1. Schematic diagram of the recombination model under steady-state condition. All of the quantities are defined in the context.

where n, p, and n_x are the densities of free electrons, free holes, and free excitons, respectively; n_c is the characteristic concentration of the material systems and also related to dimensionality. For two dimensions it is given by

$$n_c=\frac{\mu k_b T}{\pi\hbar^2}\exp(-E_x/k_B T), \tag{2}$$

where μ is the reduced mass and E_x is the excitonic binding energy. Thus n_c is the strong function of temperature T.

As the recent experiments pointed out, nonradiative recombination channels are usually introduced and play a significant role in recombination dynamics of free excitons and free carriers in semiconductor quantum wells at higher temperature. In this case, the decay of photoexcited carriers is the consequence of both radiative and nonradiative recombination. It is implied that two kinds of carriers are distinguished in the overall photogenerated carriers. One is those which decay radiatively through the states of free excitons and free electron-hole pairs, and the other decay nonradiatively through deep levels and mediate states, as shown in Fig. 1. Therefore both radiative and nonradiative fractions should be included in the electronic neutrality condition and particle conservation. Under the steady-state condition, we then have

$$\Delta n_x+\Delta p=N_0-N_{\rm nr}=N_{\rm rad}, \tag{3}$$

where $\Delta n_x=n_x-n_{x0}$, $\Delta p=\Delta n=p-p_0$ are the excess densities of free excitons and free carriers, respectively; N_0 is the total number (density) of carriers trapped by the active region, i.e., the quantum well, after the continuous-wave photoexcitation or injection; $N_{\rm rad}$ and $N_{\rm nr}$ are the radiative and nonradiative fractions, respectively. By solving Eq. (1) and Eq. (3), we obtain the relative population of free excitons for n-type materials in terms of radiative fraction $N_{\rm rad}$

$$r_x\equiv\frac{\Delta n_x}{N_{\rm rad}}=1-\frac{n_0+n_c}{2N_{\rm rad}}\left\{\left[1+\frac{4n_c N_{\rm rad}}{(n_0+n_c)^2}\right]^{1/2}-1\right\}, \tag{4}$$

where n_0 is the background (majority) concentration inside the well. The relative population of free carriers is then $r_{\text{e-h}}=1-r_x$. For simplicity, the temperature-independent n_0 is assumed hereafter since a slow variation of n_0 with temperature mainly due to thermal ionization of impurities outsides the well is usually negligible by comparison with n_c.

With both radiative and nonradiative recombination taken into account, the rate equation of the overall density inside the well can be written as

$$\frac{dN}{dt}=\frac{N}{\tau_{\rm rad}}+\frac{N}{\tau_{\rm nr}}, \tag{5}$$

where $\tau_{\rm rad}$ is the overall radiative recombination lifetime including recombinations of both free excitons and free carriers; $\tau_{\rm nr}$ is the nonradiative recombination time constant. From the rate equations of free excitons and free carriers in the quantum wells, $\tau_{\rm rad}^{-1}=\tau_x^{-1}+Bn_c$. Here τ_x is the excitonic lifetime and B is the band-to-band recombination coefficient.

According to Eq. (5), the radiative fraction in terms of overall density N_0 is given by

$$N_{\rm rad}=\frac{\tau_{\rm nr}}{\tau_{\rm rad}+\tau_{\rm nr}}N_0. \tag{6}$$

The total quantum efficiency η of the quantum well related to the radiative fraction is determined by

$$\eta=\frac{N_{\rm rad}}{N_0}=\frac{\tau_{\rm eff}}{\tau_{\rm rad}}, \tag{7}$$

where $\tau_{\rm eff}^{-1}=\tau_{\rm rad}^{-1}+\tau_{\rm nr}^{-1}$ is the decay time constant of photoluminescence intensity which can be measured experimentally.

Based on the fact that PL intensity is proportional to the product of the number of particles and the corresponding radiative recombination rate, we have

$$I_x\propto\tau_x^{-1}\Delta n_x, \tag{8}$$

where I_x stands for the excitonic PL intensity. In the regime of low excitation, Eq. (4) can be further simplified and gives

$$\Delta n_x=\frac{N_{\rm rad}}{1+(n_c/n_0)}=\frac{N_0}{[1+(n_c/n_0)][1+(\tau_{\rm rad}/\tau_{\rm nr})]}. \tag{9}$$

Equation (9) is valid only if $N_{\rm rad}\ll\max(n_0,n_c)$, where the notation $\max(x,y)$ denotes the maximum between x and y. Based on Eqs. (8) and (9), the simple but clear relationships of excitonic PL intensity with temperature and excitation intensity are obtained in the regime of low excitation.

$$I_x=\frac{\beta}{[1+(n_c/n_0)][1+(\tau_{\rm rad}/\tau_{\rm nr})]}I_0, \tag{10}$$

where β is the coefficient representing overall collection efficiency of photoexcited carriers including photon absorption and the carrier transport from the outside barriers into the well.

The temperature dependence of the nonradiative channels is typically characterized by $\tau_{\rm nr}^{-1}=\Gamma_0^{-1}\exp(-E_A/k_B T)$. Γ_0 is the scattering time constant. The constant nonradiative

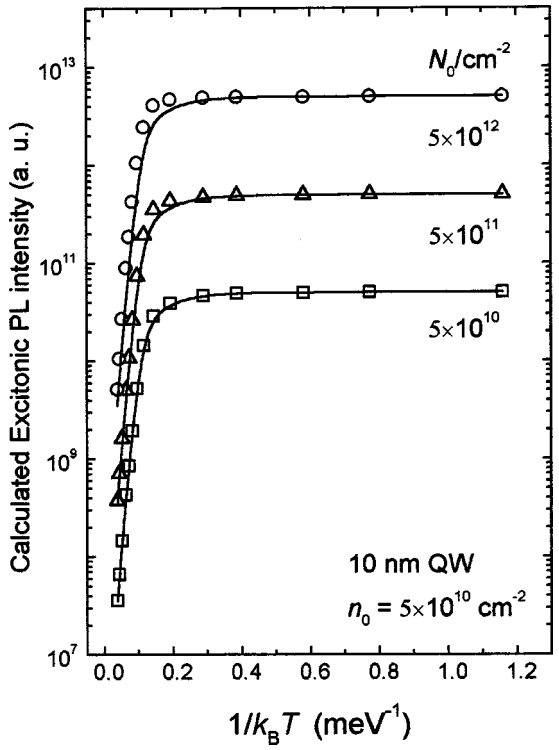

FIG. 2. Comparison between the calculated excitonic PL intensity (□, △, and ▽) and low-excitation approach (solid lines) under various excitation intensities.

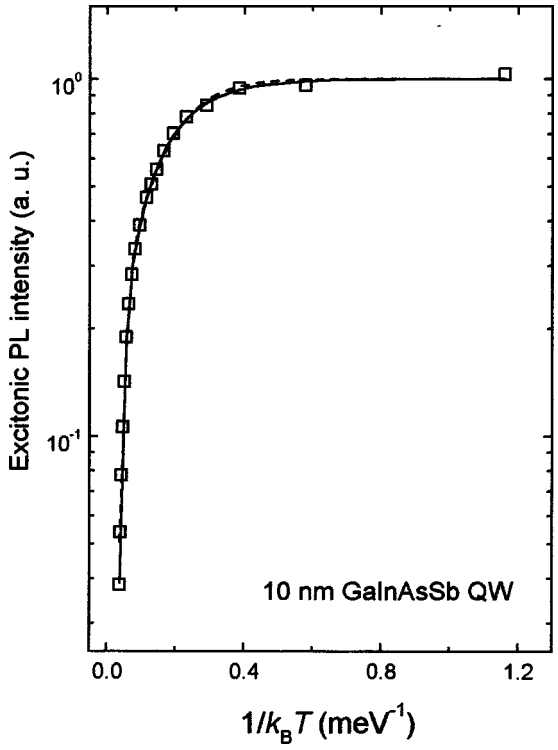

FIG. 3. The Arrhenius plot of excitonic PL intensity (□), best fit curves according to Eq. (11) (solid line) and the upper fit function in Table I (dashed line).

term has been neglected for high quality samples. The temperature dependence of τ_{rad} is mainly determined by the excitonic lifetime τ_x, which can be approximated by the simple expression $\tau_x = \gamma_0 k_B T$.[1,16,17] Therefore two distinct thermal processes correlated to excitonic recombination are clearly demonstrated according to the two terms in the denominator of Eq. (10). One is attributed to the thermal ionization of free excitons into free carriers. The other is the activation of nonradiative channels which appears at higher temperature. Based on the above discussion, the fitting function with the four parameters is suggested as

$$\frac{1}{\beta}\left(\frac{I_x}{I_0}\right)(x=1/k_BT)=\left[\left(1+\frac{P_1}{x}\exp(-P_2x)\right)\times\left(1+\frac{P_3}{x}\exp(-P_4x)\right)\right]^{-1}. \quad (11)$$

Using Eqs. (2) and (10), we have the relations as follows: $P_1=\mu/\pi\hbar^2 n_0=1.47\times10^{10}/n_0(\mathrm{cm}^{-2})$ for GaInAsSb/GaAlAsSb quantum wells, $P_2=E_x$, $P_3=\gamma_0/\Gamma_0$, $P_2=E_A$. All four fitting parameters are uniquely related to the material and characteristic parameters, respectively.

III. CALCULATIONS AND COMPARISON WITH EXPERIMENTS

Figure 2 displays the calculated accurate exciton PL intensity and its low-excitation approach according to Eq. (10) as a function of temperature. A good agreement is found even when the excitation density is close to the background value. This strongly suggests that the low-excitation approach of Eq. (10) is available for most of the measurements we considered. The calculated overall PL intensity is also provided in the figure. The larger intensity difference between the overall PL and excitonic PL is found at higher temperatures, which results from the thermal ionization of excitons, but their temperature behaviors are the same. However, as stated above, due to both larger radiative recombination lifetime and smaller relative population of band-to-band recombination of free carriers, the measured PL approximates to excitonic PL rather than computed overall PL in the low temperature range for most quantum well structures.

We next describe and discuss our experimental results. The samples studied are $Ga_{0.76}In_{0.24}As_{0.02}Sb_{0.98}/Ga_{0.82}Al_{0.18}As_{0.02}Sb_{0.98}$ single quantum well structures with a well thickness of 10 nm, grown by solid source molecular-beam epitaxy. The photoluminescence was taken with a Nicolet 760 Fourier transform IR spectrometer with 1 cm^{-1} resolution with tunable sample temperature from 6.5 to 300 K. The 514.5 nm line from Ar^+ laser was used for continuous-wave excitation. The PL signal from the sample was detected by the liquid-nitrogen cooled InSb detector. Sharp and strong PL peak is observed in the whole temperature range we measured. The low-temperature ($T<100$ K) luminescence is identified as excitonic mission. Above 100 K, we find some contribution of free-carrier recombination to the PL. The excitonic contribution, however, predominates by at least one order of magnitude. For more precision, the spectrally integrated excitonic PL was made to the exclusion of the free-carrier fraction using a line-shape analysis.

TABLE I. Fit parameters which are extracted from the fit of the Arrhenius plot of excitonic PL intensity using the different functions.

Fitting function y $(x=1/k_BT)$	Fit parameters			
	P_1	P_2	P_3	P_4
$[1+P_1\exp(-P_2x)+P_3\exp(-P_4x)]^{-1}$	3.42	10.3	187	71
$\left[\left(1+\frac{P_1}{x}\exp(-P_2x)\right)\left(1+\frac{P_3}{x}\exp(-P_4x)\right)\right]^{-1}$	0.265	5.84	6.7	106

The Arrhenius plot of exciton PL intensity is plotted in Fig. 3. The fitting of the experimental data using Eq. (11) is close to perfect and much better than any fit which can be achieved using the other fitting function concerned. Table I gives all of the four parameters obtained according to the two different fit functions. The typical function used in the previous studies[18,19] is also presented for comparison. The main difference between these two fitting functions is that the parallel rather than serial recombination channels are assumed in our model. We find that the first fit function gives much larger excitonic binding energy but smaller activation energy than that of our model. From the four parameters, some results are obtained as follows: $n_0=5.5\times10^{16}$ cm^{-3}, $E_x=5.8$ meV, $\gamma_0/\Gamma_0=6.7$, $E_A=106$ meV. The fit parameter n_0 is close to the value of 5×10^{16} cm^{-3} in GaInAsSb epilayers with the same growth conditions measured by Hall experiments. Assuming that the excitonic lifetime is of several hundred picoseconds in GaInAsSb well, then the scattering time Γ_0 comes out to be about several tens of picoseconds.

In conclusion, the fundamental relationship of the excitonic PL intensity in semiconductor quantum wells has been derived. A new fit function related to the two thermal processes is proposed according to the simplified expression of excitonic PL intensity in the low excitation regime. We found that each of the four fitting parameters feature the distinct property of the sample materials and the validity has been confirmed using our experiments.

ACKNOWLEDGMENT

The authors would like to acknowledge the technical support from Professor A. Z. Li and also Y. L. Zheng for the growth of the samples.

[1] J. Feldmann, G. Peter, E. O. Göbel, P. Dawson, K. Moore, C. Foxon, and R. J. Elliott, Phys. Rev. Lett. **59**, 2337 (1987).
[2] B. K. Ridley, Phys. Rev. B **41**, 12 190 (1990).
[3] U. Cebulla, G. Bacher, A. Forchel, G. Mayer, and W. T. Tsang, Phys. Rev. B **39**, 6257 (1989).
[4] R. Eccleston, B. F. Feuerbacher, J. Kuhl, W. W. Rühle, and K. Ploog, Phys. Rev. B **45**, 11 403 (1992).
[5] Y. Takahashi, S. Owa, and S. S. Kano, Appl. Phys. Lett. **60**, 213 (1992).
[6] J. P. Bergman, P. O. Hoiltz, B. Monemar, J. L. Mrz, and A. C. Gossard, Phys. Rev. B **43**, 4765 (1991).
[7] G. Bacher, C. Hartmann, H. Schweizer, T. Held, G. Mahler, and H. Nickel, Phys. Rev. B **47**, 9545 (1993).
[8] D. S. Chemla, D. A. B. Miller, P. W. Smith, A. C. Gossard, and W. Wiegmann, J. Quantum Electron. **QE-20**, 165 (1984).
[9] I. Bastard, *Wave Mechanics Applied to Semiconductor Heterostructures* (Wiley, New York, 1991), p. 269.
[10] E. F. Schubert and W. T. Tsang, Phys. Rev. B **34**, 2991 (1986).
[11] M. Colocci, M. Gurioli, and A. Vinattieri, J. Appl. Phys. **68**, 2809 (1990).
[12] S. R. Jin and A. Z. Li, J. Appl. Phys. **81**, 7357 (1997).
[13] M. Gurioli, J. Martinez-Pastor, M. Colocci, C. Depairs, B. Chastaingt, and J. Massies, Phys. Rev. B **46**, 6922 (1992).
[14] J. D. Lambkin, D. J. Dunstan, K. P. Homewood, L. K. Howard, and M. T. Emeny, Appl. Phys. Lett. **57**, 1986 (1990).
[15] P. Michler, T. Forner, V. Hofsäβ, F. Prins, K. Zieger, F. Scholtz, and A. Hangleiter, Phys. Rev. B **49**, 16 632 (1994).
[16] L. C. Andreani, F. Tassone, and F. Bassani, Solid State Commun. **77**, 641 (1991).
[17] J. Martinez-Pastor, A. Vianttieri, L. Carraresi, M. Colocci, Ph. Roussignol, and G. Weimann, Phys. Rev. B **47**, 10 456 (1993).
[18] S. Iyer, S. Hegde, A. Abul-Fadl, K. K. Bajaj, and W. Mitchel, Phys. Rev. B **47**, 1329 (1993).
[19] J. D. Lambkin, L. Considline, S. Walsh, G. M. O'Connor, C. J. McDonagh, and T. J. Glynn, Appl. Phys. Lett. **65**, 73 (1994).